Nanoscale

COMMUNICATION

Mimicking the bioelectrocatalytic function of recombinant CotA laccase through electrostatically self-assembled bioconjugates

Received 00th January 20xx,
Accepted 00th January 20xx

DOI: 10.1039/x0xx00000x

www.rsc.org/

David Alba-Molina,[a] Daily Rodríguez-Padrón,[b] Alain R. Puente-Santiago,[b*] Juan J. Giner-Casares,[a] María T. Martín-Romero,[a] Luis Camacho,[a] Lígia O. Martins,[c] Mario J. Muñoz-Batista,[b] Manuel Cano[a*] and Rafael Luque[b,d*]

Unprecedent 3D nanobiosystems composed of recombinant CotA lacccases and citrate-stabilised gold nanoparticles have been succesfully achieved by an electrostatic self-assembly strategy. The bioelectrochemical reduction of O_2 driven by CotA laccase at the spore coat was mimicked. Consequently key insights of its bioelectrocatalytic function were unravelled.

The hierarchical arrangement of multiple building blocks to form complex structures with specific functionalities, from well-ordered protein aggregates to more sophisticated nanomachines like nucleosomes and ribosomes, is often observed in Nature.[1-5] Such well-organized biological structures can be found performing vital functions in the cells such as protein synthesis, genome packing, cellular structural support, information storage and regulation of metabolic reactions.[6,7] As a result, the building of artificial self-assembled nanostructures to mimic the function of natural systems has become an attractive research topic in the last years.[8]
Recent advances in supramolecular and synthetic chemistry have triggered the development of useful techniques towards the design of new artificial biomaterials with unique properties.[9-13] Up to now, a wide range of strategies have been developed to construct well-organized nanostructures from the self-assembly of nanoparticles and proteins as principal building blocks for a myriad of applications such as drug delivery,[14] drugs design[15] and biocatalysis.[16] With this aim, electrostatic self-assembly has been successfully used to achieve CdSe-ZnS quantum dot bioconjugates[17] and protein-ArgNPs superstructures,[18] among others.[19,20]

Multicopper oxidases (MCOs) are a family of metalloenzymes that couple the one-electron oxidation of a variety of substrate molecules, both inorganic and organic, to with four-electron reduction of dioxygen to water. These enzymes are distinguished by having three distinct copper sites, Cu types 1, 2 and 3; the oxidation of the reducing substrate occurs at the type 1 (T1) Cu site while the reduction of O_2 occurs at the T2/T3 trinuclear cluster. Specifically, CotA laccase, is a bacterial MCO that is abundant in outer coat layer of spores of the soil bacterium *Bacillus subtilis*.[21] Spores are cellular structures designed to resist a wide-range of physical-chemical extremes such as wet and dry heat, desiccation, radiation and UV light. Although CotA-laccase exact function within the spore coat is still not fully understood, it was proposed its involvement in the formation of the spore brown pigment that contribute to spore resistance against UV-light and hydrogen peroxide.[22] Particularly, it has been shown that spore coat components of marine Bacillus species promote, using molecular oxygen, the oxidation of Mn^{2+} by a biologically catalysed process.[23] Consequently, the analysis of the bioelectrochemical oxygen reduction processes on 3D-nanobiomimetic systems composed of recombinant CotA laccases and AuNPs can shed light over the catalytic function of these metalloenzymes in spore coat. The aforementioned systems are taking a core-shell configuration where enzymes are disposed along the nanoparticles surfaces that in turn simulate the spore coat shape.

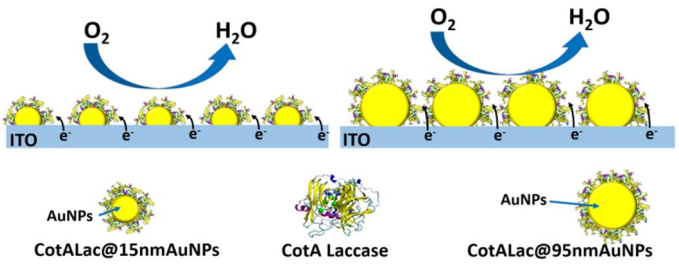

Scheme 1. Overview of the direct bioelectrocatalytic reduction of oxygen by the electrostatically self-assembled nanobioconjugates.

[a] *Departamento de Química Física y T. Aplicada, Instituto Universitario de Investigación en Química Fina y Nanoquímica IUIQFN, Facultad de Ciencias, Universidad de Córdoba, Campus de Rabanales, Ed. Marie Curie, E-14071 Córdoba, Spain. Email: q82calum@uco.es*
[b] *Departamento de Química Orgánica, Instituto Universitario de Investigación en Química Fina y Nanoquímica IUIQFN, Facultad de Ciencias, Universidad de Córdoba, Campus de Rabanales, Ed. Marie Curie, E-14071 Córdoba, Spain. Email: rafael.luque@uco.es, z02pusaa@uco.es*
[c] *Instituto de Tecnologia Química e Biológica António Xavier, Universidade Nova de Lisboa Av da Republica, 2780-157, Oeiras, Portugal.*
[d] *Peoples Friendship University of Russia (RUDN University), 6 Miklukho-Maklaya str., 117198, Moscow, Russia*

Nanoscale

COMMUNICATION

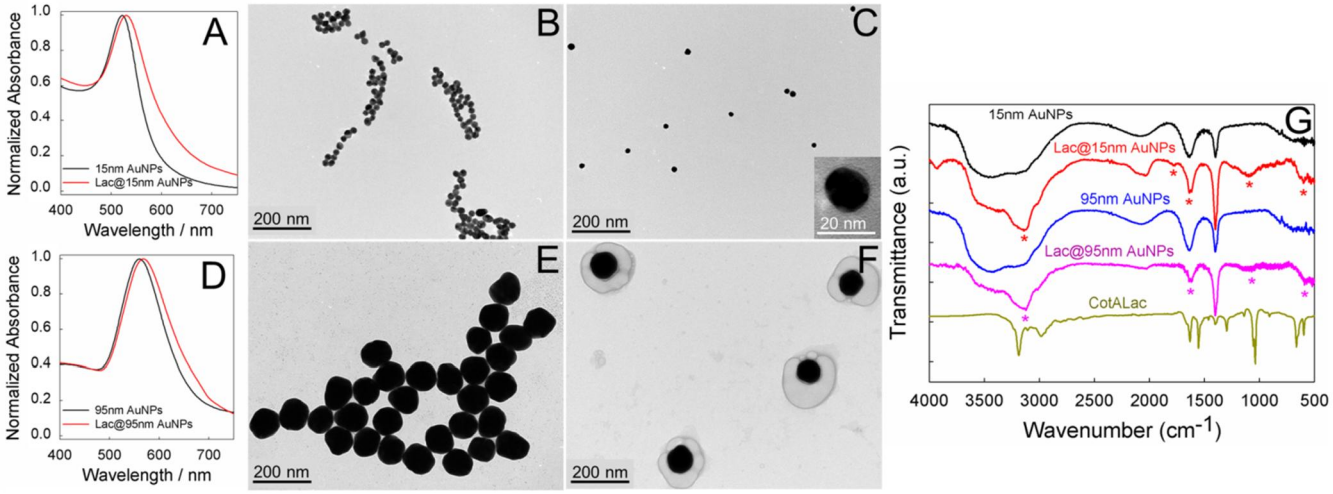

Fig. 1. **(A)** UV-visible spectra of 15nmAuNPs and its bioconjugate CotALac@15nmAuNPs. **(B and C)** TEM images of 15nmAuNPs and its bioconjugate CotALac@15nmAuNPs, respectively. **(D)** Same as **(A)** but for 95nmAuNPs. **(E and F)** TEM images of 95nmAuNPs and its bioconjugate CotALac@95nmAuNPs, respectively. **(G)** FTIR spectra of 15nmAuNPs (black line), CotALac@15nmAuNPs (red line), 95nmAuNPs (blue line), CotALac@95nmAuNPs (pink line), and CotALac (dark-yellow line).

In this work, the recombinant CotA laccase was electrostatically attached to citrate-stabilised AuNPs of 15 nm and 95nm, respectively, at physiological pH using a simple one-pot electrostatic self-assembly approach (Scheme 1). To the best of our knowledge, this is the first time that the bioelectrocatalytic function of CotA laccase is mimicked by electrically active 3D nanobioarchitectures and linked to the nanoparticles size, ionic environment and temperature effects. The isoelectric point (pI) of the CotA laccase is 7.7[24] and the overall charge of the enzyme surface is positive at neutral pH, which facilitates its electrostatic anchorage onto the negatively charged citrate groups of the AuNPs. Indeed, citrate groups can provide not only suitable 3-D platforms for tethering enzymes, but also a flexible linker to trigger the electronic communication between the redox biomolecules and the gold nanoparticles.[25] Additionally, the electrostatic self-assembly was achieved from solution allowing thus the full coverage of the nanoparticles. This strategy differs from previuos reports where laccases were immobilised onto AuNP-covered electrodes.[26]

UV-vis measurements were carrried out to determine the effects of the enzyme immobilization on the surface plasmon resonance (SPR) bands of the gold nanoparticles. Figure 1A,D displays the UV-vis spectra of the unbonded AuNPs as well as the corresponding electrostatically assembled biocojugates CotALac@15nmAuNPs and CotALac@95nmAuNPs. It can be noted a slight shift of the SPR bands of both AuNPs from 600nm to 610 nm upon the immobilization process. These results indicate a change in the dielectric nature surrounding of the metal surface nanoparticles driven by the possible salt-bridges mediated interactions (i.e. combination of two non-covalent interactions: hydrogen- and ionic-bonding) between AuNPs and enzymes as well as the maintenance of a relatively good dispersity of the nanoparticles.[27] The similar wavelenght up-shifts observed for both bioconjugates suggest a similar protein layer thickness surrounding the nanoparticles surfaces. The absence of agglomeration and the efficient enzyme coating after bioconjugation were confirmed by TEM analysis (Fig. 1 B-F). The resulting TEM images of the particles, before and after the electrostatic self-assembly process, showed no variation in Au-core size and shape but with a significant variation in their protein-corona, which was especially evident in CotALac@95nmAuNPs (Fig. 1F).

The immobilization of CotA laccase was confirmed by FT-IR (Figure 1G). AuNPs, with both 15 nm and 95 nm particle sizes, showed the typical carboxylate bands of the citrate coating, such as asymmetric C=O stretching (1641 cm^{-1}) and symmetric C-O stretching (1400 cm^{-1}).[28] FT-IR spectra of CotALac@15nmAuNPs and CotALac@95nmAuNPs exhibited the presence of amide I vibrations (C=O stretch and C-N in-plane bending) overlapped with carboxylate ones. The appearance of a double peak (1639 and 1619 cm^{-1}) can be attributed to C=O stretching from Amide I and asymmetric C=O stretching from carboxylate groups, respectively. On the other hand, significance changes in intensity of the peak at 1400 cm^{-1} can be assigned to a combination of C-N in-plane bending from Amide I and symmetric C-O stretching from carboxylate groups.[29]

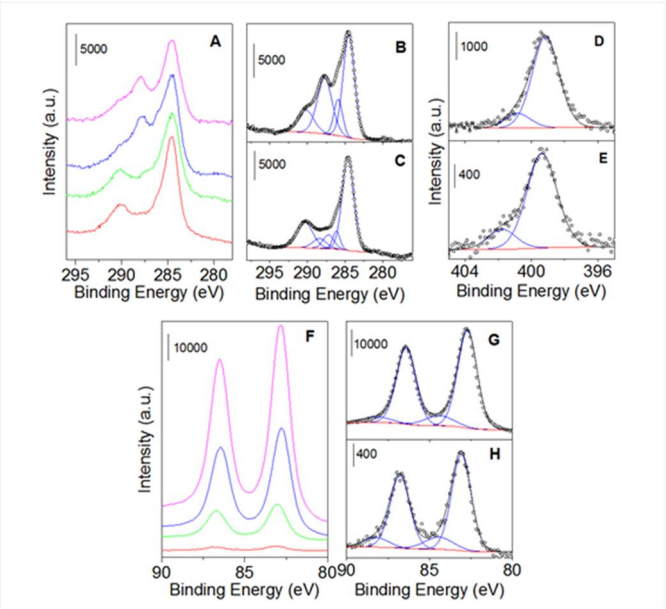

Fig. 2. (A) XPS spectra of the prepared bioconjugates for C1s; Deconvoluted high-resolution C1s XPS spectra of **(B)** 15nmAuNPs and **(C)** CotALac@15nmAuNPs; Deconvoluted high-resolution N1s XPS spectra of **(D)** CotALac@95nmAuNPs and **(E)** CotALac@15nmAuNPs; **(F)** XPS spectra of the prepared bioconjugates for Au4f, Deconvoluted high-resolution Au4f XPS spectra of **(G)** CotALac@95nmAuNPs and **(H)** CotALac@15nmAuNPs 95nm AuNPs (pink line), 15nmAuNPs (blue line), CotALac@95nmAuNPs (green line) and CotALac@15nmAuNPs (red line).

Also, both bioconjugates presented C-O-C (1102 cm^{-1}) and C-C (600 cm^{-1}) stretching modes observed in pristine CotA laccase spectra. These observations clearly confirmed the presence of CotA laccase in the coating. Surprisingly, amide II band of the CotA laccase, which is located at 1554 cm^{-1}, dissappeared upon the immobilization step for both bioconjugates suggesting the existance of an interaction between the N-H groups of the enzymes and the carboxylate groups of the citrate capped AuNPs.[30] Although the amide I band contribution of both bioconjugates retained the same positions in comparison to the free-CotA laccase, the absence of the amide II bands clearly suggest that the enzymes underwent slight conformational changes due to the salt-bridges interactions between the carboxylate groups of the citrate-stabilized AuNPs and the amine and/or quaternary ammonium groups of the CotALaccase.[30]

The formation of both bioconjugates was also monitored by Dynamic Light Scattering (DLS) and Zeta-Potential (ZP) measurements (Table S1). As it was expected for the electrostatic adsorption of enzyme molecules to AuNPs surface, DLS analysis showed an increase in the hydrodynamic diameters (HD) of the particles after bioconjugation. Considering the given HD of the CotALac and assuming a slight variation of the hydration shell of the AuNPs, the resulting bioconjugate volumes indicate both, the formation of a monolayer of CotA laccase molecules and the absence of aggregation during the self-assembly process. In addition, ZP analysis displayed a decrease of the surface charge of the particles after bioconjugation. A similar behaviour was recently reported after conjugation of Rhus vernicifera laccase to negatively charged AuNPs by using a non-covalent binding approach.[31]

XPS measurements were performed in order to fully understand the chemical properties of the prepared nanomaterials, as well as, to corroborate the successful protein immobilization on the nanoparticles surface. The obtained spectra revealed the presence of C, Au and O for all the samples. Particularly, XPS analysis of the protein modified materials showed a band around 399 eV, which can be assigned to N1s, confirming the effectiveness of the functionalization process. N1s spectra of both CotALac@95nmAuNPs and CotALac@15nmAuNPs (Figure 2D-E) displayed two contributions associated to N from peptide bonds and pyrimidinic groups. In addition, not Au–N coordination was observed, since it is well known that N1s binding energy decreases by 1–3 eV upon binding to metallic surfaces due to a transfer of electron density from nitrogen to metals.[32] Deconvoluted high-resolution C1s XPS spectrum of 15nmAuNPs (Figure 2B) exhibited four well-defined contributions at 284.6, 285.9, 287.9 and 290.2 eV, which can be attributed to C-C/C=C, CH_2-COH, COO-(Au) and COO-(H), respectively. In turn, C1s XPS spectrum of CotALac@15nmAuNPs (Figure 2C) can be deconvoluted in five peaks at 284.6, 286.2, 287.2, 288.1 and 290.3 eV, related to C-C/C=C, CH_2-COH, C-N, COO-(Au) and COO-(H), respectively.[25] Specially, the band at 287.2 eV corroborated the successful protein immobilization. It is also worth to mention that the relative intensity of the peak assigned to COO-(Au), consistent with the presence of citrate coordination to Au surface, decreases for the laccase functionalized nanoparticles, most likely due to the salt-bridge mediated interaction of the protein with the citrate groups (contributing to the C-N peak) and partial citrate displacement after the immobilization process.[33] Furthermore, high-resolution XPS spectra of the Au 4f core level exhibited two peaks around 82.9 and 84.4 eV from Au(0) and Au(I), respectively, suggesting that the dominant oxidation state of gold in the samples is Au(0), with minimal charge transfer at the citrate/AuNPs interface.[34] Noticeably, the N/Au ratio was determined for both CotALac@95nmAuNPs and CotALac@15nmAuNPs, being 4 times higher for CotALac@15nmAuNPs than for CotALac@95nmAuNPs (protein content higher for functionalized 15nmAuNPs, Table S2).

The electrocatalytic properties toward the reduction of oxygen of the CotA laccases, CotALac@15nmAuNPs and CotALac@95nmAuNPs deposited onto ITO electrodes, were subsequently evaluated by cyclic voltammetry (Figure 3). Free-CotA laccases exhibited a poor electrocatalytic activity (Figure 3B) most probably due to unsuitable orientations of the enzymes onto the ITO surfaces towards the electroreduction of oxygen, which adopt mainly a random orientation.[35] On the other hand, when the redox biomolecules were electrostatically anchored to gold nanoparticles, remarkable electrocatalytic currents were observed (Figure 3D). These

results suggest that AuNPs allow the direct electron transfer (DET) of the enzymes, act as efficient electronic bridges between the proteins and the surface electrodes, provide active ET orientations and thus greatly enhance their bioelectrocatalytic performances. It is well-established that the difference in the electrocatalytic behaviour of redox enzymes is driven by their orientation distribution patterns. A random distribution of enzyme orientation commonly leads to low electrocatalytic signal[36] whereas the immobilization of proteins at highly oriented active ET configurations produces excellent bioelectronic yields.[37] Rudiger et al. have proved that both orientation and electrocatalytic properties of enzymes bearing a dipole moment can be controlled by electrostatic interactions at the protein/amino-terminated monolayer interfaces.[38] Since CotA laccase exhibits two well-defined positively and negatively charged regions at the surface (Figure S2), it can adopt, after the electrostatic attachment, a preferential orientation resulting in efficient ET configurations, with a very positive impact on their bioelectrocatalytic activities.

Also, the apparent midpoint potential ($E^{o'}$) of the resulting bioconjugates in N_2-saturated sodium phosphate buffer (50 mM, pH 7.0) were -0.156V and -0.154 V for CotALac@15nmAuNPs and CotALac@95nmAuNPs, respectively, more negative as compared to -0.072 V, the value obtained for the free-CotA laccase (Figure 3A and 3C). This result could be understood by the influence of the negatively charged surface nanoenvironment of the citrate groups.[39-41] Interestingly, enzymes immobilized onto the smallest nanoparticles delivered higher electrocatalytic currents indicating that the nanometric dimensions of the AuNPs provides an extra-improvement of the electrostatically tied enzyme DET reaction rate. Such remarks are in good agreement with the Antonio D. Lacey et al. work, where laccases were covalently attached to gold nanoparticles of 5 and 16 nm respectively, following an oriented immobilization approach.[26] On the opposite trend, Sergey Shleev et al. concluded by strong experimental evidences that bioelectrocatalytic reaction rates do not changes with particle sizes of the gold nanoparticles in the 20-80nm range.[42]

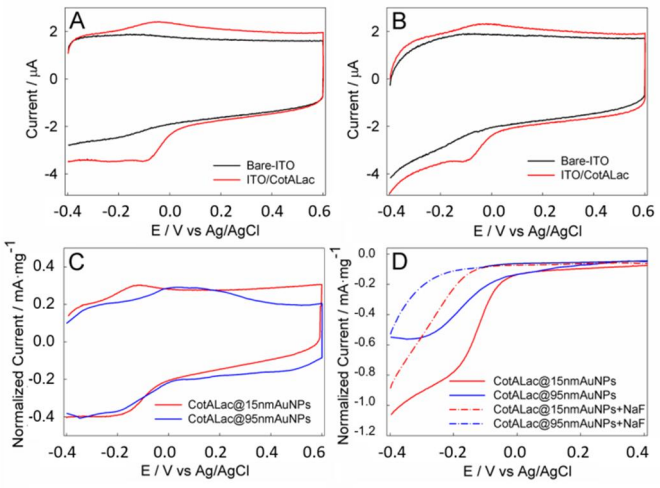

Fig. 3. Cyclic voltammograms (CVs) of Bare-ITO and ITO electrode modified with pristine CotALac in N_2-saturated **(A)** and O_2-saturated **(B)** sodium phosphate buffer (50 mM, pH 7.0). **(C)** CVs of ITOs modified with CotALac@15nmAuNPs and CotALac@95nmAuNPs in N_2-saturated sodium phosphate buffer (50 mM, pH 7.0). **(D)** CVs of ITOs modified with CotALac@15nmAuNPs and CotALac@95nmAuNPs in O_2-saturated sodium phosphate buffer (50 mM, pH 7.0) in the absence or presence of NaF (30 mM). Scan rate, 100 mV·sec^{-1}.

In order to explain the influence of the nanoparticle size on the bioelectrocatalytic performances of CotA laccase-citrate capped AuNPs bionanostructures, we propose the following ideas. Firstly, the bioelectrocatalytic features of each electrically active nanobioarchitecture is strongly related with the particular methodology used to synthesized the pristine nanostructures as well as the immobilization approach used to anchor the redox enzymes. In these sense, it is worth to point out that spherical character of the nanoparticles suffers a significant decreasing at larger sizes using our synthetic approach.[43] Therefore, it could be expected a lesser organization of the citrate layer structure at the smallest nanoparticles due to the increase of the nanoparticles curvature, which in fact may induce some disorganization on the citrate nanodomains as described in various works for monolayer-protected gold nanoparticles.[44] Bearing in mind these facts, CotA laccases immobilized onto disordered citrate nanodomains of the 15 nm AuNPs can more easily penetrate and accommodate their redox sites closer to the electrodes surfaces and consequently improve both the DET responses and the enzymatic bioelectrocatalytic yields.

The pronounced shifting toward negative potentials of the onset potential values of the CotA laccase immobilised on citrate-stabilised gold nanoparticles (0.005 V (vs Ag/AgCl)) is remarkable compared with the values of 0.60 V and 0.37V (vs Ag/AgCl) obtained for fungus and recombinant laccases immobilized on carbon nanotubes (CNTs), respectively.[45,46] The remarkable changes in the onset potential of the CotALac@AuNPs can be explained by the structural and functional differences among the enzymes and/or the singular nanoenvironmental conditions created by the citrate groups at the enzymes/AuNPs interfaces.[45, 47]

The influence of halides ions over the electrocatalytic activity of laccases has been widely investigated to provide additional insights into their ET pathways. It is well known that fluoride anions binds to T2/T3 trinuclear copper center and supress the intramolecular ET (IET) from the type 1 copper centre (T1) to the T2/T3 Cu cluster.[48] In order to obtain a deeper understanding of the prepared nanobiomimetic systems, the electrocatalytic behaviour of the biocojugates were assessed upon the addition of 30 mM of NaF, which in fact have never been investigated so far. Surprisingly, the electrocatalytic activity of the CotA laccases (Figure 3D) did not drastically changes in the presence of NaF, in strong contrast with previous works where a totally hindered of the bioelectrochemical reduction of O_2, even at very low

concentrations (1-30 mM), was observed.[49,50] At the same time, onset potentials shifted to -0.11 V for both bioconjugates, which constitute a very unusual performance of laccases exposed to fluoride anions solutions. This is in accordance with the seminal work of Marius Dagys et al., which have elegantly demonstrated that the electronic wiring of laccases to gold nanoparticles takes place via T2/T3 Cu cluster instead of T1 redox sites, with the trinuclear copper centre facing the electrode surfaces, bypassing the intramolecular electron transfer, which under certain conditions is the rate-limiting step of oxygen bioelectroreduction.[51] Thus, the unusual electrocatalytic behaviour of the CotALac@AuNPs bioconjugates may be related to the effective electronic connection of CotA laccases to citrate stabilised AuNPs via the T2/T3 Cu redox center.

Finally, we have conducted electrocatalytic experiments at 60^{o}C taking into account the high thermophilic character of the CotA laccases[21] (Figure S3). At this temperature the bioelectrocatalytic activity of the bioconjugates significantly dropped likely due to a partial break-up of the electrostatic interactions between the enzymes and the AuNPs.

This work opens the doors towards the development of laccase-based nanobioelectrocatalytic materials constructed by electrostatic self-assembly methodology. To deeply study the salt-bridges interaction in our systems, it could be interesting to address in future works the electrostatic or enthalpy-driven nature of these types of interactions following previous protein-protein binding studies.[52]

Conclusions

A mimicking of the CotA laccase bioelectroctalytic function in the spore coat components was successfully accomplished through the formation of a full monolayer of metalloenzymes onto citrate-coated AuNPs, lead by attractive electrostatic interactions. Such interactions can modulated the orientation of the enzymes an in turn their bioelectrocatalytic performances. Noteworthy, the onset potential values of the bioconjugates for the bioelectrochemical reduction of O_2 were very close to 0V (0.005V), which suggest that CotA Laccase need low overpotentials in spore coat to reduce molecular oxygen and participate in enzymatic physiological processes, giving support for the location and function of an oxidoreductase in the thickest spore coat layer where the diffusion of oxygen is hampered. Interestingly, the electronic wiring of the enzymes is likely produced via a T2/T3 trinuclear with the T2/T3 redox groups facing the electrodes surfaces. This work paves the way towards the design of new nanobioelectrocatalytic systems for a deeper understanding of the biological structure and function of recombinant metalloenzymes.

Acknowledgements

Rafael Luque gratefully acknowledges MINECO for funding project CTQ2016-78289-P, co-financed with FEDER funds. Daily Rodriguez-Padron and Alain R. Puente-Santiago gratefully acknowledge MINECO for their research contracts associated to the aforementioned project. Alain R. Puente-Santiago also acknowledges to COST FP1306 (LignoVal, http://www.cost.eu/COST_Actions/fps/FP1306) for support under an STSM short stay in the lab of Prof. Ligia O Martins and to the Research Program of the University of Cordoba for its financial support through a postdoctoral contract (Modality 5.1). Mario J. Munoz-Batista gratefully acknowledges MINECO for a JdC contract (Ref. FJCI-2016-29014). J.J.G.-C. acknowledges the Ministry of Economy and Competitiveness for a "Ramon y Cajal" contract (#RyC-2014-14956) and the project CTQ2017-83961-R. M. C. thanks the "Plan Propio de Investigación" from the Universidad de Córdoba and the "Programa Operativo de fondos FEDER Andalucía" for its financial support through a postdoctoral contract (Modality A).

References

1. P. Fratzl and R. Weinkamer, *Prog. Mater. Sci.*, 2007, **52**, 1263-1334.
2. G. M. Whitesides and B. Grzybowski, *Science*, 2002, **295**, 2418-2421.
3. Y. S. Bai, Q. Luo and J. Q. Liu, *Chem. Soc. Rev.*, 2016, **45**, 2756-2767.
4. J. Zhou, X. W. Du, C. Berciu, H. J. He, J. F. Shi, D. Nicastro and B. Xu, *Chem*, 2016, **1**, 7-9.
5. J. A. Marsh, H. Hernandez, Z. Hall, S. E. Ahnert, T. Perica, C. V. Robinson and S. A. Teichmann, *Cell*, 2013, **153**, 461-470.
6. Q. Luo, C. X. Hou, Y. S. Bai, R. B. Wang and J. Q. Liu, *Chem. Rev.*, 2016, **116**, 13571-13632.
7. D. S. Goodsell and A. J. Olson, *Annu. Rev. Biophys. Biomol. Struct.*, 2000, **29**, 105-153.
8. H. C. Sun, Q. Luo, C. X. Hou and J. Q. Liu, *Nano Today*, 2017, **14**, 16-41.
9. K. Kinbara and T. Aida, *Chemical Reviews*, 2005, **105**, 1377-1400.
10. S. G. Zhang, *Nat. Biotechnol.*, 2003, **21**, 1171-1178.`
11. C. E. Zhao, J. S. Wu, S. Kjelleberg, J. S. C. Loo and Q. C. Zhang, *Small*, 2015, **11**, 3440-3443.
12. R. B. Song, Y. C. Wu, Z. Q. Lin, J. Xie, C. H. Tan, J. S. C. Loo, B. Cao, J. R. Zhang, J. J. Zhu and Q. C. Zhang, *Angew. Chem. Int. Ed.*, 2017, **56**, 10516-10520.
13. V. B. Wang, J. Du, X. F. Chen, A. W. Thomas, N. D. Kirchhofer, L. E. Garner, M. T. Maw, W. H. Poh, J. Hinks, S. Wuertz, S. Kjelleberg, Q. C. Zhang, J. S. C. Loo and G. C. Bazan, *Phys. Chem. Chem. Phys.*, 2013, **15**, 5867-5872.
14. F. Scaletti, J. Hardie, Y. W. Lee, D. C. Luther, M. Ray and V. M. Rotello, *Chem. Soc. Rev.*, 2018, **47**, 3421-3432.
15. N. Serna, L. Sanchez-Garcia, A. Sanchez-Chardi, U. Unzueta, M. Roldan, R. Mangues, E. Vazquez and A. Villaverde, *Acta Biomater.*, 2017, **60**, 256-263.
16. M. Holdrich, A. Sievers-Engler and M. Lammerhofer, *Anal. Bioanal. Chem.*, 2016, **408**, 5415-5427.
17. H. Mattoussi, J. M. Mauro, E. R. Goldman, G. P. Anderson, V. C. Sundar, F. V. Mikulec and M. G. Bawendi, *J. Am. Chem. Soc.*, 2000, **122**, 12142-12150.
18. R. Mout, G. Y. Tonga, L. S. Wang, M. Ray, T. Roy and V. M. Rotello, *ACS Nano*, 2017, **11**, 3456-3462.

19. Y. C. Yeh, R. Tang, R. Mout, Y. Jeong and V. M. Rotello, *Angew. Chem. Int. Ed.*, 2014, **53**, 5137-5141.
20. C. M. Yu, Y. D. Wang, L. Wang, Z. K. Zhu, N. Bao and H. Y. Gu, *Colloids Surf. B Biointerfaces*, 2013, **103**, 231-237.
21. F. J. Enguita, L. O. Martins, A. O. Henriques and M. A. Carrondo, *J. Biol. Chem*, 2003, **278**, 19416-19425.
22. L. O. Martins, P. Durao, V. Brissos and P. F. Lindley, *Cell. Mol. Life Sci.*, 2015, **72**, 911-922.
23. J. P. M. Devrind, E. W. Devrinddejong, J. W. H. Devoogt, P. Westbroek, F. C. Boogerd and R. A. Rosson, *Appl. Environ. Microbiol.*, 1986, **52**, 1096-1100.
24. L. O. Martins, C. M. Soares, M. M. Pereira, M. Teixeira, T. Costa, G. H. Jones and A. O. Henriques, *J. Biol. Chem*, 2002, **277**, 18849-18859.
25. E. Koposova, G. Shumilova, Y. Ermolenko, A. Kisner, A. Offenhausser and Y. Mourzina, *Sens. Actuator B-Chem.*, 2015, **207**, 1045-1052.
26. C. Gutierrez-Sanchez, M. Pita, C. Vaz-Dominguez, S. Shleev and A. L. De Lacey, *J. Am. Chem. Soc.*, 2012, **134**, 17212-17220.
27. Y. Liu, R. L. Mernaugh and X. Q. Zeng, *Biosens. Bioelectron.*, 2009, **24**, 2853-2857.
28. J. W. Park and J. S. Shumaker-Parry, *J. Am. Chem. Soc.*, 2014, **136**, 1907-1921.
29. E. Mueller and A. Blume, *Biochim. Biophys. Acta*, 1993, **1146**, 45-51.
30. A. Kowalczyk, E. Matysiak-Brynda, M. Bystrzejewski, D. S. Sutherland, Z. Stojek and A. M. Nowicka, *Acta Biomater.*, 2016, **45**, 367-374.
31. M. P. de Almeida, P. Quaresma, S. Sousa, C. Couto, I. Gomes, L. Krippahl, R. Franco and E. Pereira, *PCCP*, 2018, **20**, 16761-16769.
32. D. Curry, A. Cameron, B. MacDonald, C. Nganou, H. Scheller, J. Marsh, S. Beale, M. S. Lu, Z. Shan, R. Kaliaperumal, H. P. Xu, M. Servos, C. Bennett, S. MacQuarrie, K. D. Oakes, M. Mkandawire and X. Zhang, *Nanoscale*, 2015, **7**, 19611-19619.
33. G. S. Perera, S. A. Athukorale, F. Perez, C. U. Pittman and D. M. Zhang, *J. Colloid Interface Sci.*, 2018, **511**, 335-343.
34. H. Al-Johani, E. Abou-Hamad, A. Jedidi, C. M. Widdifield, J. Viger-Gravel, S. S. Sangaru, D. Gajan, D. H. Anjum, S. Ould-Chikh, M. N. Hedhili, A. Gurinov, M. J. Kelly, M. El Eter, L. Cavallo, L. Emsley and J. M. Basset, *Nat. Chem.*, 2017, **9**, 890-895.
35. A. Franco, S. Cebrián-García, D. Rodriguez-Padron, A. R. Puente-Santiago, M. Muñoz-Batista, A. Caballero, A. M. Balu, A. A. Romero and R. Luque, *ACS Sustain. Chem. Eng.*, 2018, **6**, 11058-11062.
36. G. A. Huerta-Miranda, A. A. Arrocha-Arcos and M. Miranda-Hernandez, *Bioelectrochemistry*, 2018, **122**, 77-83.
37. M. Bourourou, K. Elouarzaki, N. Lalaoui, C. Agnes, A. Le Goff, M. Holzinger, A. Maaref and S. Cosnier, *Chem. Eur. J.*, 2013, **19**, 9371-9375.
38. O. Rudiger, J. M. Abad, E. C. Hatchikian, V. M. Fernandez and A. L. De Lacey, *J. Am. Chem. Soc.*, 2005, **127**, 16008-16009.
39. L. L. Xue, Y. H. Wang, Y. Xie, P. Yao, W. H. Wang, W. Qian, Z. X. Huang, J. Wu and Z. X. Xia, *Biochemistry*, 1999, **38**, 11961-11972.
40. J. Zhou, J. Zheng and S. Y. Jiang, *J. Phys. Chem. B*, 2004, **108**, 17418-17424.
41. A. R. Puente-Santiago, D. Rodriguez-Padron, Xuebo Quan, M. J. Muñoz Batista, L. O. Martins, S. Verma, R. S. Varma, J. Zhou and R. Luque, *submitted to Energy Environ.Sci.*
42. D. Pankratov, R. Sundberg, D. B. Suyatin, J. Sotres, A. Barrantes, T. Ruzgas, I. Maximov, L. Montelius and S. Shleev, *RSC Adv.* 2014, **4**, 38164-38168.
43. N. G. Bastus, J. Comenge and V. Puntes, *Langmuir*, 2011, **27**, 11098-11105.
44. J. C. Love, L. A. Estroff, J. K. Kriebel, R. G. Nuzzo and G. M. Whitesides, *Chem. Rev.*, 2005, **105**, 1103-1169.
45. J. Atalah, Y. Zhou, G. Espina, J. M. Blamey and R. P. Ramasamy, *Catal. Sci. Technol.*, 2018, **8**, 1272-1276.
46. F. Wu, L. Su, P. Yu and L. Q. Mao, *J. Am. Chem. Soc.*, 2017, **139**, 1565-1574.
47. S. Shleev, A. Jarosz-Wilkolazka, A. Khalunina, O. Morozova, A. Yaropolov, T. Ruzgas and L. Gorton, *Bioelectrochemistry*, 2005, **67**, 115-124.
48. T. Beneyton, Y. Beyl, D. A. Guschin, A. D. Griffiths, V. Taly and W. Schuhmann, *Electroanalysis*, 2011, **23**, 1781-1789.
49. S. Holmberg, M. Rodriguez-Delgado, R. D. Milton, N. Ornelas-Soto, S. D. Minteer, R. Parra and M. J. Madou, *ACS Catal.*, 2015, **5**, 7507-7518.
50. M. Dagys, K. Haberska, S. Shleev, T. Arnebrant, J. Kulys and T. Ruzgas, *Electrochem. Commun.*, 2010, **12**, 933-935.
51. M. Dagys, A. Laurynenas, D. Ratautas, J. Kulys, R. Vidziunaite, M. Talaikis, G. Niaura, L. Marcinkeviciene, R. Meskys and S. Shleev, *Energy Environ. Sci.*, 2017, **10**, 498-502.
52. K. Okazaki, T. Sato and M. Takano, *J. Am. Chem. Soc.*, 2012, **134**, 8918-8925.

